Conference Proceedings

EuroSun 2016
Palma de Mallorca (Spain), 11 – 14 October 2016

11th ISES EuroSun2016 – Design and Dynamic Simulation of a Small Multipurpose Solar Thermal System for Rural Necessities

Simone Amicabile[1], Christophe Hick[2], Surendranath Yagnamurthy[3], Mattia Roccabruna[1], Ankit Dev[4], Luigi Crema[1]

[1] ARES Unit, Fondazione Bruno Kessler, 38123 Povo, Trento (Italy)

[2] University of Liège, Campus du Sart Tilman - Bat: B49 - P33 4000 Liège (Belgium)

[3] Indian Institute of Technology, Hauz Khas, New Delhi, Delhi 110016 (India)

[4] Indian Institute of Technology Roorkee, Haridwar Highway, Roorkee, Uttarakhand 247667 (India)

Abstract

The proposed paper explains in detail the sizing process and dynamic simulation of a solar powered system designed to satisfy the energy demand of a school in the rural area of Haridwar district, India. The system is able to satisfy heterogeneous power demands for typical rural applications: hay pasteurization process, refrigerated storage for vegetables (explained in a second publication) and steam cooking. The considered layout is first described and evaluated under steady state assumption to identify the rough size of the main components. The specific configuration is then implemented and simulated using a Modelica-based layout, specifically developed for the case study. The dynamic behaviour of the system for different power requirements is simulated and analyzed over a typical day of usage. The goal to properly size and study the solar field, Phase Change Material (PCM) thermal storage and overall Balance Of Plant (BOP) is achieved.
Simulations results show that an optimal sizing can be achieved despite the large area of solar collectors required to ensure the power requirements of the facility. A better trade off between economic investment and system effectiveness can be accomplished slightly shifting the daily cooking activities.
The final designed system is going be implemented and commissioned in the proposed rural area. Future work will consist in comparing experimental data with the dynamic model predictions.

Keywords: CSP, Solar cooking, Solar cooling, Solar hay processing, Dynamic modeling, Dymola.

doi:10.18086/eurosun.2016.04.08 Available at http://proceedings.ises.org

Nomenclature

P&I	Pipe and Instruments
CSP	Concentrated Solar Power
PCM	Phase Change Material
BOP	Balance Of Plant
GDP	Gross Domestic Product
INR	Indian Rupees
ITPAR	India Trento Program for Advanced Research
Δh_{EVAP}	Delta enthalpy of vaporization
η_{POT}	Efficiency of the cooking pot system
CPC	Compound Parabolic Collectors
PTC	Parabolic Through Collectors
DNI	Direct normal Irradiation
θincid	Solar Incident angle
Tamb	Ambient temperature
Vwind	Wind speed
$\dot{q}_{tot,t}$	Total thermal energy transfer
$\dot{q}_{tot,g}$	Thermal energy transfer to the glass
$\dot{q}_{rad,air}$	Energy transfer to the ambient ait
η_{opt}	Optical efficiency
A_{ref}	Solar reference area
$A_{ext,g}$	External glass collector area
ϵ_g	Glass emissivity
σ	Boltzman's constant
$T_{ext,g}$	Glass external temperature
T_{sky}	Sky temperature
M_W	Wall mass
N	Discretization number
c_W	Heat capacity of the wall
T_W	Wall temperature
$\dot{q}$	Thermal heat transfer
A_{int}	Internal surface
U_l	Liquid heat transfer coefficient
U_{tp}	Two-phases heat transfer coefficient
U_v	Vapour heat transfer coefficient
$\varepsilon_{is,P}$	Pump isentropic efficiency
c_0, c_1, c_2, c_n	Non-dimensional constants
$\mathbf{f}_{\mathbf{P}}^{*}$	Pump frequency
$\mathbf{r}_{\mathbf{p,P}}^{*}$	Pressure ration
Δp	Pressure loss
k	Friction factor
ρ	Fluid density
A	Cross sectional area
$\dot{V}$	Volumetric flow rate

1. Introduction

India is the second most populated country in the world, almost 1.3 billion of people (Worldmeter, 2016) with more than 50% below the age of 25 and more than 65% below the age of 35 (BBC report, 2007). The astonishing population growth over the past 20 years can be mainly attributed to a remarkable economic growth, which placed the country among the 10 largest economies in the world by nominal Gross Domestic Product (GDP) (IMF, 2014). Economic progress made significant changes all around this vast nation, both in cities and minor villages, with a remarkable effect on the life style and habits of millions of people.

This rapid change eventually created strong disparities between rural and metropolitan areas. The signs of this important gap can be easily found in many aspects of people's daily life.

While most part of the Indian cities and central villages can base their daily activities on a reliable and stable electric power distribution grid, this is not liable for smaller communities. Rural areas are in fact non-uniformly electrified, depending on the financial resources of each single state. Due to this aspect, 400 million Indians are without electricity in rural India, 40% of the whole world's population without access to electricity (University of Washington, 2013). Lack of internal resources, economic poverty, and poor planning are some of the most relevant causes which has contributed to leave rural villages in India without electricity, while urban areas have experienced in the last few decades' growth in electricity capacity and consumption. In these circumstances, diesel generators fulfill the basic electric demand, which is normally used to guarantee food preservation (through refrigerators) or essential illumination. Cooking and heating necessities need also to be taken into account. In rural communities most part of the cooking activities are still accomplished through the use of traditional wood fired stoves or fossil fuels such petrol and kerosene. The dependence of rural households on traditional fuel is mainly due to the poor purchasing capacity of the people to buy commercial fuel and the easy accessibility to traditional sources like cow-dung and agricultural wastes (Kumar et al., 2010). As it is easy to expect, the thermal efficiency of these traditional sources is very low, approximately 15% (energy efficiency). The use of these traditional fuels is estimated to cause around 400,000 premature annual deaths due to various respiratory problems (NISTADS, 2008). Furthermore, the vast availability of unemployed and cheap manpower for fuel collection worsens this situation.

The government is increasingly trying to improve these harsh conditions by funding projects and initiatives related to biogas, solar and wind energy applications. Since the slow process of total electrification will perhaps take many years to provide an extended and reliable grid, alternatives, based on clean and abundant renewable energies, need to be evaluated as viable solution for small and middle size rural applications for India villages. Among the bigger programs, the Jawaharlal Nehru National (JNN) Solar Mission has the ambitious goal of implementing 20,000 MW of solar power by 2022 reducing the cost of solar power generation in the country (Ministry of new and renewable energy, 2013). The Indian government is also tying to sensitize people to clean energies. In a five-year plan, 30,000 million INR (approx. $500 million USD) are budgeted for clean cooking education in more than 500,000 schools (Wikia, 2016).

In this context, the India Trento Program for Advanced Research (ITPAR) is running the "Sustainable Technologies for distributed level Applications and energy support to Rural development" (STAR) project. ITPAR is bilateral collaboration supported by the Department of Science and Technology of the Indian Government (DST) and by the Province of Trento with the supervision of the Italian Ministry for Foreign Affairs. It involves some of the main university teams and research institutes of the Province of Trento and India. The STAR project is participated by the research institute Fondazione Bruno Kessler (FBK) from Trento, the Indian Institute of Technology (IIT) Roorkee, IIT Delhi and University South Campus Delhi. The project aims at the integration of a novel energy system in the district of Hardwar, composed of a combined solar thermal plant able to satisfy part of the daily thermal requirements of the Chudiyala Mohanpur village's high school. At the same time, the system is able to store thermal energy and run a hay processer prototype used by the village's farmers to improve the nutritional properties and quality of hay for animal feedstock.

The thermal system integrates two different technologies of solar collectors and a high capacity PCM thermal storage to decouple solar energy and thermal necessities. It is designed as demo system but it will be able to satisfy part of the energy-related necessities of the school.

The hay-processing device will be also implemented at a demonstrative size to prove the concept. In parallel, the school will be also supplied with an innovative solar cooler machine to store vegetables for short to mid

term periods. Since the analysis of this second system is beyond the scope of the paper, the description will not be included.

A preliminary system evaluation identifies energy requirements and components considering the steam requirements for the community's daily activities. After this first stage of design, the main components of the system are selected and a dynamic simulation in Modelica environment is chased with the objective of meeting collector's area and the thermal storage dimension. Figure 1 conceptually summarizes the paper structures and how the different chapters are structured and linked each other.

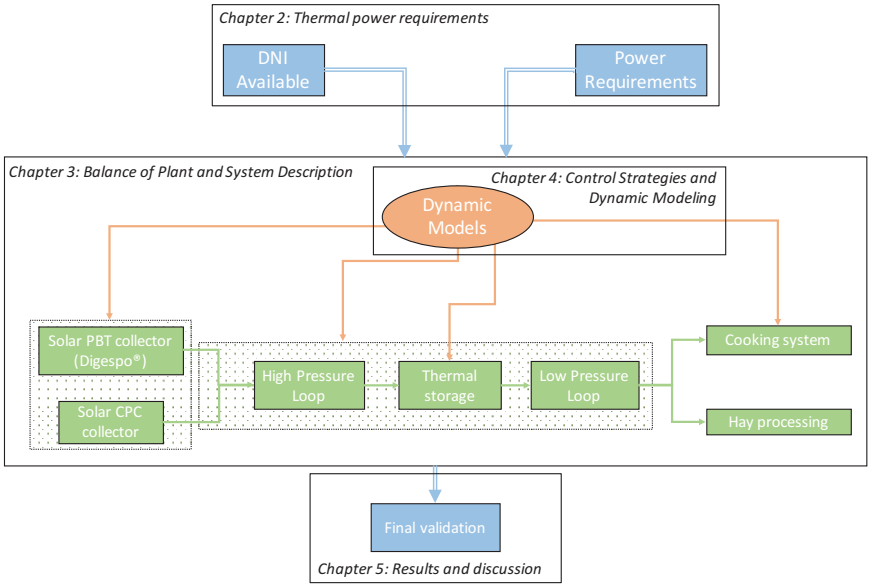

Fig. 1: Flow chart of the design development process. Inputs and outputs are highlighted in light blue. Dynamic model and P&I blocks are highlighted in orange and light greens, respectively.

2. Thermal power requirements

Within the framework of renewable energy system integrations for medium and small-size rural villages, a multi-purpose concentrated solar power (CSP) application is designed and presented. The proposed layout implements a thermal solution able to supply a reliable and clean source of thermal power. The system will be employed in a high school of an Indian rural village with a total number of about 600 people, including students and teachers.

The solar system has the initial target to demonstrate the application of the concept and further increase the size of the prototype. The researchers of the Indian Institute of Technology of Roorkee have assumed reference values for the quantity of food the system has to guarantee daily.

Assuming rice as the most common food prepared for the students, comprehensive analyses on the energy for cooking consumptions are available in literature. The studies help to estimate the energy required to cook rice, under specific assumptions such as type of cooking process, time needed and pre-treatment of the rice (Tribeni et al., 2006). Controlled energy input, cooking under pressure and soaking of rice before cooking are the three approaches that can be directly traduced into energy saving. (Dilip Kumar De et al., 2014) also chased a detail study related to the energy required for rice cooking process. According to this study, the energy consumption for fired open cooking of 1 kg of non-soaked rice requires 1.6 kg of water. Furthermore, the majority of the households in rural countries use firewood to prepare their daily meals. This process approximately needs 1.64 MJ of heat delivered to the pot. Energy cooking consumption easily varies depending on the process but values for fired open pots are reasonably similar to the ones for the discussed system (steam injected kettle). Hypotheses therefore are necessary to quantify the steam consumption on the working fluid side. Assuming that only the latent heat of vaporization/condensation of steam is transferred to the product, the delta enthalpy of vaporization for steam Δh_{EVAP} is 2326 kJ/kg. The specific heat of water is

assumed constant and equal to 4.186 kJ/kgK. Assuming a reference efficiency of the cooking system of η_{POT}: 75%, the amount of steam required to cook 10kg of rice can be estimated. Table 1 lists the constants introduced for this evaluation.

Tab. 1: Summary of the ingredients properties and total energy required for the cooking process.

Primary sources	Quantities (kg)	Heat capacities (kJ/kgK)	Total energy required (kJ)	Efficiency of the cooking pot	Total steam required for cooking (kg)
Rice	10	2.5	16400	75%	9.4
Water	1.6	4.186			

Once the energy demand of the main cooking process is identified, the power system is designed in order to fulfill the demand. The system will be opportunely oversized due to the uncertainty of some variables and assumptions such thermal losses due to poor insulation. Furthermore, the system has also to be able to provide the right amount of energy required to process the hay for the village's farmers.

3. Balance of Plant and System Description

Scheme of Figure 2 shows how the designed layout can be divided into two different main blocks. The plant has two separated loops: high pressure loop, circled within the blue line segment, and low pressure loop, highlighted in green. In the first circuit, high-pressure water is heated up close to the saturation temperature through a combination of Compound Parabolic Collectors (CPC) and an innovative Parabolic Through Collectors (PTC) technology. The proposed solution includes high efficiency CPC coupled with novel coaxial PTC, developed in the framework of the EU funded DIGESPO project (FP7-DIGESPO, grant agreement n° *241267*). Due to the high working temperature of the system, these two different technologies linked together ensure respectable values of nominal efficiency even with temperatures close to the upper limit set point. Because of this specific solution, high temperatures can be reached at the solar field outlet, ensuring good efficiency with acceptable investment costs. At the same time, high temperature energy can be stored inside the thermal storage, reducing for instance the risk of sub-cooled vapor at the low-pressure side. High-pressure loop works at nominal pressure of 10 bar (with possible maximum pressure of 12 bar). At this stage, water changes phase at approximately 179 °C, guaranteeing high temperature in the storage. The control of the solar system is implemented in order to work with a safe sub-cooling temperature of 10 °C. If outlet temperature T4 of Figure 1 overpasses the maximum temperature, a safety control defocuses the DIGESPO solar field, before emergency relief valves empty the system.
Temperature and pressure and mass flow sensors (according to the legend) are located in the most significant parts of the system.
The choice of using pressurized water instead of thermal oil is an advantage in terms of BOP simplicity and reliability. Avoiding oil allows the use of inexpensive working fluid and components, such pumps or expansion vessels. Solar collectors do not require any changes to work with pressurized water and both typologies of collectors can handle the nominal design pressure. Additionally, the maintenance cost is considerably reduced and spare components are expected to be easier to find for water or steam rather than for oil, especially in rural areas. This choice globally helps to decrease the initial investment cost as well as the maintenance of the storage system.
The final system, designed to exploit the solar thermal power for different rural applications widespread in most part of the Indian rural communities (Kuldeep Ojha, 2010), is expected to be flexible and easily scalable to increase its potential.

3.1 High-pressure loop

The high-pressure loop is composed by CPC solar collectors connected in series with PTC DIGESPO collectors. CPC field pre-heats the fluid before entering the DIGESPO collectors. In this part the fluid will reach the maximum target temperature with relatively low thermal losses. The fluid flow is regulated through variable speed pump of Figure 1, which can be tuned in order to reduce and eventually stop the flow. The pressurized loop discharges the liquid water directly inside the thermal storage. For this reason, the tank does

not have internal coil but is itself working at the same nominal pressure of the collectors. Two parallel loops are added in case the thermal storage requires maintenance or direct steam generation tests want to be carried out (see Figure 2).

3.2 Low-pressure loop

The low-pressure loop is in charge of delivering high temperature thermal energy using water at steam phase as thermal vector. In order to provide a low-pressure steam circuit, the thermal storage is built up with a finned internal coil to allow improved heat exchange between the hot pressurized water and the non-pressurized water. The expected temperature difference between the two loops (pressurized water inlet and non-pressurized water inlet) is around 100 °C. The thermal storage is filled with PCM balls in order to keep the temperature controlled inside the tank and to reduce its total dimensions.

The low-pressure distribution system, highlighted in green in Figure 2, connects this first part of circuit with all the final devices. A three-way valve allows to manually choosing whether to divert the steam flow to the hay processer or to the cooking kettle. If the steam produced is exploited through the hay processor, a reintegration of fresh water is necessary. In case the steam is used for the cooking system, no reintegration is needed since the loop is close. Despite this, a small condenser with steam trap is built-in directly in the kettle's loop to guarantee liquid phase before the feeding pump.

The feeding pump is chosen as variable speed, driving the mass flow rate in this loop. This choice is because a variable flow is able to guarantee a constant inlet temperature at the exchanger, guaranteeing the right amount and quality of steam.

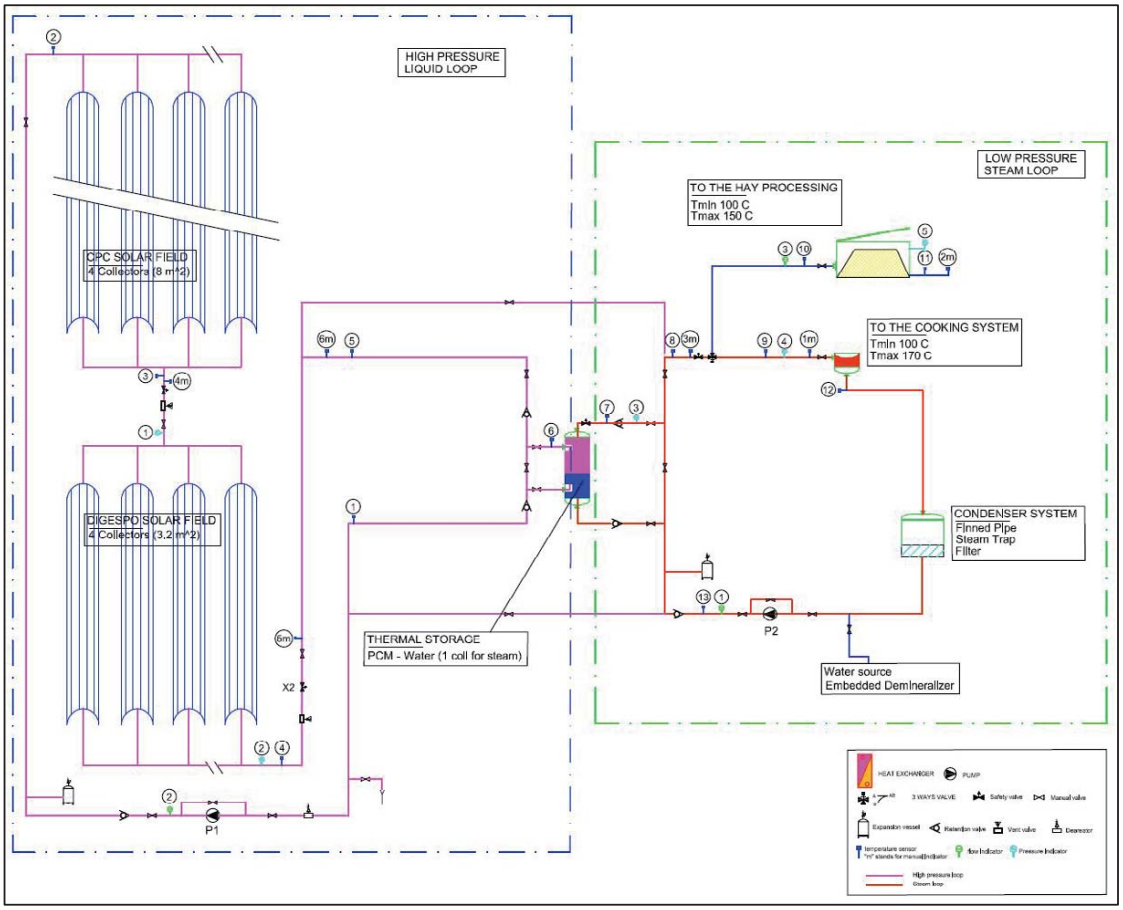

Fig. 2: BoP for the system proposed. High and Low pressure loops are highlighted in blue and green, respectively.

3.3 Thermal storage

The chart of figure 3 shows the typical DNI trend along the different seasons in the Uttarakhand sate. During the sunniest period of the year (summer season), the maximum value of DNI available in the demo site area hardly reaches 520 W/m^2. This is mainly due to the though typical weather of the region. Despite the high temperatures reached during summer season, clouds often cover sky, directly affecting the power available. Furthermore, the chart shows the irradiation distribution all along the day. The peak of power is expected around midday, when the sun is higher in the sky. This is a considerable issue for cooking applications, since they are expected to work at full load during this period of the day. The cooking system will be mainly used between 11AM and 1PM to prepare the daily meals for the school. Less problematic is the use of the hay process because it doesn't require activation during specific periods of the day. For these reasons, a thermal storage is necessary to partially decouple solar power and thermal demand. The thermal storage requires being capable to storage at least the amount of energy necessary to cook the preselected amount of food.
Since the power required for the cooking process is much higher than the power delivered through the sun, the storage will be rapidly discharged when the cooking process is active. Because of that, the dimension of the storage has to be enough large to avoid this problem. On the other hand a bigger storage could affect the maximum temperature reached.

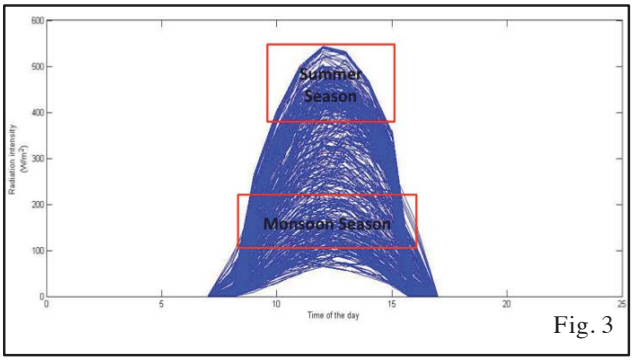

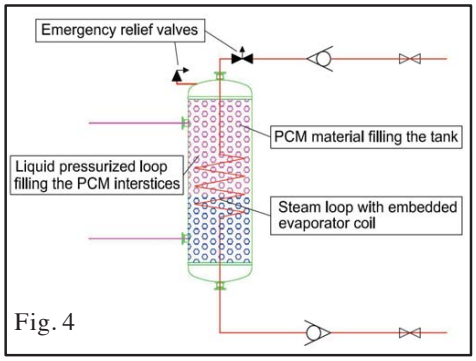

Fig. 3: Distribution of Direct Normal Irradiation (DNI) along the days of a typical year.
Fig. 4: Schematic of the pressurized thermal storage with PCM balls.

If the power available is not sufficient to charge the storage, the temperature reached could be too low to produce steam when necessary. This concern could be even more amplified with the use of PCM material inside the tank. If is true that PCM materials help reducing the total volume occupied by the storage, on the other hand the material has to reach the saturation temperature in order to change phase and to store sensible heat. If this doesn't occur, the PCM material is un-useful since only latent heat without a controlled temperature is stored. For these reasons the storage requires a careful sizing and a simplified approach to implement and study the dynamic behavior of the whole system is pursued. Figure 4 briefly describes how the storage is designed. The phase change material fill the pressurized vessel and the water coming from the solar field will fill the interstices among each ball. In this way the heat power will be directly exchanged between fluid and metal balls containing the PCM. The pressurized tank has a built-in coil connected to the low-pressure steam loop to provide the power only when necessary through the use of a variable speed pump.

3.4 Solar collectors

The designed system is characterized by two different kinds of collectors: CPC and PTC DIGESPO tubes. Parabolic through collectors with evacuated tubular absorber are renown as the most reliable technology in the Concentrated Solar Power (CSP) field (Cabello et al., 2011). In the proposed system, the CPC solar field works as a pre-heater for the CSP collectors, reducing the global investment cost of the solar field. CPC collectors have high reliability ensuring a good compromise between efficiency and capital cost.
CPC collector field is connected in series to the higher temperature DIGESPO technology collectors. This

second stage has the fundamental role to increase the temperature up to the maximum temperature before going directly to the thermal storage to heat up the PCM material. An external glass tube and an internal metallic support compose the evacuated solar tube developed within the DIGESPO project. The metallic support is tubular while an absorber pipe made from stainless steel had been specifically realized with a molybdenum protection layer and coated with CerMet. The potential problem arising from thermal stress dilation and glass cracks has been solved with the use of a coaxial tube. A spiral wire is present between the two coaxial pipes solving the thermal gradient problems and reducing thermal deformations. The full-evacuated solar tube has an inner diameter of 12 mm and a total length of 2 meters for an active surface of 0.8 m^2. The solar technology has been fully proven on a demonstration site. The solar plant prototype was installed in Malta, supplying thermal energy for industrial heat processes. The solar collector's efficiency reached 55% with DNI of 900 W/m^2 and working temperature of 300°C. Due to the noticeable efficiency that the collectors are able to show at high temperature, is reasonable to expect that the thermal losses related to the last stage of the solar field will be considerably low compare to a solution made by CPC collectors only.

3.5 Cooking system and hay processing

The low-pressure system delivers the steam directly to the steam-cooking kettle, a device specifically designed to use steam as thermal vector. The typical steam kettles are large container with a round or spherical bottom. Kettles have a double wall or "jacket" covering the bottom and at least half of the height of the sides, to provide space for steam to circulate thereby heating the cooking surface. In principle, the steam kettle operates like the classic kitchen double boiler. The kettle operates within a specific pressure range at which the steam can be injected into the kettle. This range is typically between 0,07 Bar and 3,5 Bar with nominal temperature up to 150°C. The kettle used for this application is 100-liter capacity SS304 kettle. The outlet part of the kettle is provided with steam safety valve and condenser system, including air vent, Y type strainer and steam trap.

Through a three-way valve, the steam coming from the PCM tank can be diverted to the hay processer when cooking demand is absent. The process for which the steam is involved is to pasteurize wheat straw without complete sterilize the cereal. Unlike sterilization, pasteurization is simply the process by which amounts of microscopic competitors in a substrate are reduced (IDFA, 2016). Sterilization in fact, would remove all living organisms, leaving the straw without beneficial bacteria and therefore susceptible to contaminants. As consequence, having beneficial microorganisms allows inoculating the straw without using special sterile procedures. Pasteurization generally occurs between 70-75° C but it is strongly dependent by the thermal death point of fungus or spores. Due to the scientific aspect of the system will be implemented, a maximum temperature up to 150°C is required for the hay processer. Steam temperature and exposure time are crucial components of this process.

4. Control Strategies and Dynamic Modeling

The control strategies for the system is developed and simulated using thermal daily requirements of the elementary school coupled with yearly weather data of the specific geographical area. Weather data are available at (Weather Data Reference, 2012).

The typical trend of thermal requirements for food cooking and hay processing is represented in the chart of Figure 5. Here, the simulated power requirements used for the dynamic simulation are depicted with time dependency.

At the very beginning of a typical day, thermal demand is absent since neither cooking stoves or hay system is activated. This is considered as small advantage for the system, which is therefore able to cumulate the solar energy available the early hours of the morning before cooking activities begin. At 11AM the school kitchen starts to warm up the circuits with high temperature steam. At this stage the power requirement is much higher then what instantly available from the solar field. For this reason, the lack of power is fulfilled through the thermal storage system.

The cooking energy requirement of 7 kWh can be reasonably approximated constant for one hour, between 11.30AM and 12.30AM when the school activities are still on going. This is approximately happening the

whole year, with exception for the monsoon season, which lasts from June to early September. During this period in fact, thermal cooking requirements are absent and the system will be completely dedicated to produce steam for hay processing or different sporadic activities requiring steam, such sterilization or cleaning. Outside the monsoon season, the hay process thermal requirements are satisfied during the afternoon period. Since this action does not need to respect strict schedule as the school lunchtime, hay processing activities are simulated as two sessions requiring 2, 5 kWh energy (including extra energy due to thermal inertia) for one hour each. This choice allows the system having enough time to store energy inside the thermal tank after the cooking period. This strategy has been developed and selected among different proposals and it will be implemented at the first stage of the on-field tests.

In order to forecast and study the transient behavior of the whole layout during the proposed typical day, a Modelica based system has been simulated with Dymola environment using the thermodynamic library ThermoCycle. ThermoCycle is an open-source Modelica Library (Modelica Website, 2016). This is a powerful tool able to describe in details the dynamic behavior of complex thermodynamic systems thanks to a user-friendly and widely tunable interface. (Desideri et al., 2015).

The model is first used to complete the design of the layout and to properly size the embedded thermal storage indispensable to decouple solar energy from power demand.

In Figure 6, the Dymola layout describing the implemented system is presented.

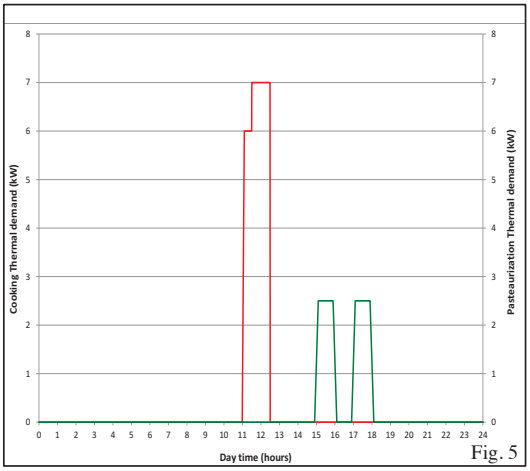

Fig. 5

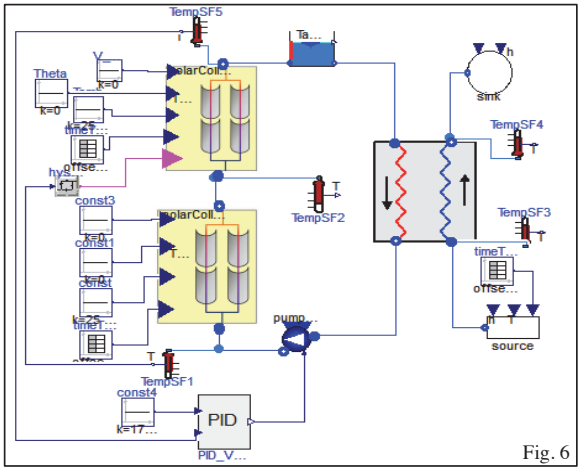

Fig. 6

Fig. 5: Scheduled thermal requirements of the system for both hay processing and cooking.
Fig. 6: Overview of the system layout implemented with Dymola.

High-pressure, liquid phase water is simulated inside the solar system while the evaporation process is modeled on the heat distribution part, right side of Figure 6. The water going to the storage tank warms up the phase change material to produce superheated steam through a dedicated boiling system. The steam loop is designed as open loop that delivers the power provided by the solar plant directly to the final users.

The dynamic modelling is necessary to define the size of the main components of the system as well as the reactiveness of the layout to rapid changes of working conditions. In addition, the dynamic model tests if safe working conditions in terms of maximum pressure and temperatures are guaranteed.

4.1. Dymola modeling: Solar collectors

Assuming homogeneous pressure drop and equal ambient input data, the solar field can be modeled as a single CPC collector in series with four PTC DIGESPO type collectors arranged in parallel. For this particular connection, the mass flow inside each single PTC collector is one fourth of the total mass flow. Parabolic through collector model of *ThermoCycle* library is used. Given the ratio between the diameter and the length of the parabolic through unit, the modeling approach is based on a finite volume one-dimensional discretization along the collector axial axis. The model is the result of two subcomponents. *Flow1Dim* component models the fluid flow through the Heat Collector Element (HCE) accounting for energy and mass transfer. At the same time, thermal inertia in the HCE is accounted by the *MetalWall* and *SolAbs* models as

depicted in Figure 7. Moreover, the model implements the relations between the environmental parameters (DNI, θ_{incid} , T_{amb} , V_{wind}) and the axial temperature distribution along the absorber. The equations defining the thermal energy transfer from the sun energy concentrated on the heat collector element to the heat transfer fluid are listed below. The first equation describes the thermal energy transfer from the sun to the metal wall of the absorber (refer to nomenclature table):

$$\dot{q}_{tot,t} = \frac{DNI \cdot \eta_{opt,t} \cdot A_{ref}}{A_{ext,t}} \quad \text{(eq. 1)}$$

Thermal energy transfer from the sun to the glass envelope:

$$\dot{q}_{tot,g} = \frac{DNI \cdot \eta_{opt,g} \cdot A_{ref}}{A_{ext,g}} \quad \text{(eq. 2)}$$

Radiation to the ambient air:

$$\dot{q}_{rad,air} = \epsilon_g \cdot \sigma \cdot (T^4_{ext,g} - T^4_{sky}) \quad \text{(eq. 3)}$$

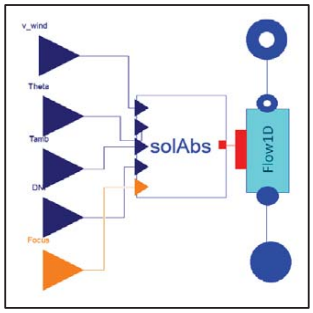

Fig. 7: Solar collector model available on ThermoCycle library.

4.2 Dymola modeling: PCM storage

A PCM tank is a major component for most part of the solar power plants due to its capacity to storage thermal energy for short and medium periods of time (Casati et al., 2013). The PCM storage of this study is modeled using three discretized one-dimensional subcomponents of the *ThermoCycle* library. Two *Flow1Dim* components accounting for mass and energy exchange in the two separated coils are merged with the PCM*Wall* component, which accounts for the overall energy accumulated in metal coils, metal balls containing the PCM and in the water filling tank. *PCMWall* component derives from the basic *MetalWall* component available on Modelica. *MetalWall* generally accounts for thermal energy accumulation in the metal wall. In this study this component has been modified in order to describe the typical thermodynamic behavior of PCM materials. The models are discretized based on the finite volume approach as depicted in Figure 8. No pressure losses are considered in the two *Flow1Dim* models and the temperature in the storage is supposed to be homogenous for each layer. Thermal energy accumulation is expressed as:

$$\frac{M_w}{N \cdot c_w} \cdot \frac{dT_w}{dt} = A_{ext} \cdot \dot{q}_{ext} + A_{int} \cdot \dot{q}_{int} \quad \text{(eq. 4)}$$

where M_w is the total mass of the wall, N is the number of cells and c_W is the heat capacity. The secondary fluid is modelled as an incompressible fluid whose density and specific heat capacity are assumed constant throughout the exchanger length. The component has been modified in order to consider the latent heat during the transition phase of the PCM at the specific temperature of 150°C. The computation of the heat transfer coefficient for the PCM storage and more generally for all the heat exchangers of the dynamic system, is based on a structure taking advantage of the object-oriented Modelica language. The basic interface, define an ideal heat transfer element with no thermal resistance. The object takes as an input the

bulk state of the fluid and computes the thermal energy flow per area.

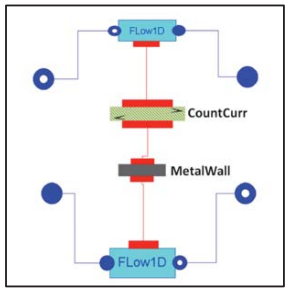

Fig. 8: Representation of the finite volume heat transfer basic block.

Based on these considerations, equation 4 is used to model convective heat transfer coefficient accounting for mass flow variation (refer to nomenclature table):

$$U = \frac{(U_l + U_{tp} + U_v)}{3} \left(\frac{\dot{m}}{\dot{m}_{nom}}\right)^n \quad \text{(eq. 5)}$$

where the exponent n varies depending on the flow regime between 0.65 and 0.8.

4.3 Dymola modeling: Cooking system

Three different models from ThermoCycle library compose the cooking pot model. *Flow1Dim* describes the steam flow through the cooking pot while *MetalWall* model is used to consider the thermal inertia of the device's metal wall. The last component takes into account the heat transfer between the steam and the food. Inputs for the final component are the food quantity and the cooking time to assess the power extraction considering constant convective and radiative ambient losses.

4.4 Dymola modeling: Pump, pressure drop, bypass valve and PID

The *Pump* model of *ThermoCycle* library is used to simulate the pump units installed on the system. It is a lumped fictitious model simulating the compression of a fluid in a turbo or volumetric machine, where given the flow fraction or the pump frequency, a constant volumetric and isentropic efficiency, the mass flow and the consumed power are computed (Desideri et al., 2015). The isentropic efficiency is simulated in Eq. 6 with a second order polynomial with cross terms as a function of the non-dimensional pressure ratio ($r^*_{p,P}$), and the non-dimensional pump frequency (f^*_P).

$$\varepsilon_{is,P} = c_0 + c_1 \cdot f_P^* + c_2 \cdot (f_P^*)^2 + c_3 \cdot r_{p,P}^* + c_4 \cdot (r_{p,P}^*)^2 + c_5 \cdot f_P^* \cdot r_{p,P}^* \quad \text{(eq. 6)}$$

$$\Delta p = \Delta p_{linear} + \Delta p_{quadratic}; \quad \Delta p_{linear} = k \cdot \dot{V}; \quad \Delta p_{quadratic} = \frac{1}{A^2} \cdot \frac{\dot{m}^2}{2 \cdot \rho} \quad \text{(eq. 7)}$$

A linear and quadratic pressure drop terms are used to compute the total pressure drop, as depicted in equation 7. *Valve* model from the *ThermoCycle* library is also a lumped model where no dynamic and thermal energy losses to the ambient are considered.

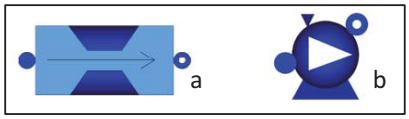

Fig. 9: (a) Pressure losses modelica block. (b) Ideal pump modelica block.

5. Results and Discussion

Four different configurations are simulated over the period of 24 hours and presented with the intention of properly address the solar field and energy storage sizing. A typical averaged day of the summer season has been identified to exploit the simulations. Phase change transitions directly affect the complexity of the simulations. For this reason only daily simulations can be performed at this stage of the study. During the worse season of the year, which is identified in as the monsoon season, the system will be totally deactivated; therefore there is no real necessity to perform simulations with the lowest irradiation values.
Each of the following charts presented includes the selected DNI used for the Dymola simulations. The solar system is composed of two different parts. Four DIGESPO parabolic through collectors for a total constant area of 3.2 m^2 and a CPC assembly, with a variable total collector area. An extensive study can become interesting if considering a future potential cost reduction of the DIGESPO collectors involving local manufacturing or large-scale production.
To summarize, the four scenarios describe the behaviour of the system changing the PCM total mass and the CPC collector area. The PCM change phase temperature equal to 150°C allows choosing among a wide range of phase change materials available on the market (Haillot et al., 2010).
Each simulation is described through two charts. Charts a) of each figure describes the trend of energy storage in the PCM tank as function of time and power demand (blue trend line). The systems starts in the morning at the storage tank lowest temperature set point of 140°C. In order to correctly estimate the actual size of the energy reserve, the reference value of the energy stored is set at 0 kWh for the simulation starting point. Charts b) of the four tests show the trends of the working steam temperature available at the thermal storage outlet and the average storage temperature.

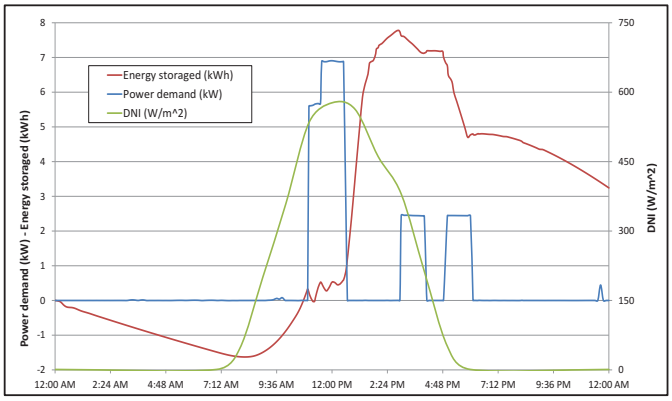

Fig. 10: Scenario 1_Power demand and energy available in the PCM storage

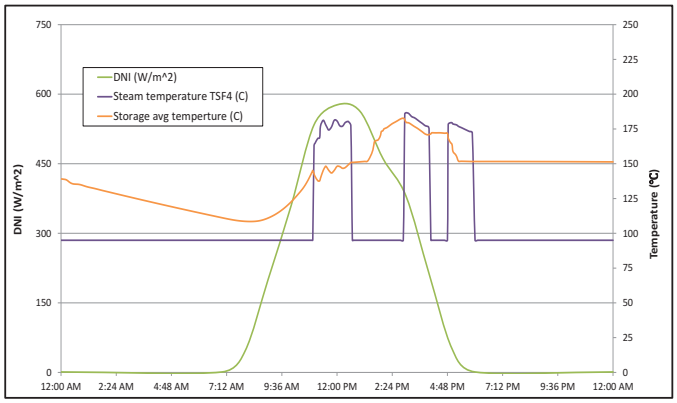

Fig. 11: Scenario 1_ Temperatures of supplied steam and tank average temperature over daily time.

Figure 10 describes the first scenario modelled shows interesting results regarding the potentiality of the thermal storage. This test is characterized by collector areas of 12 m^2 and 3.2 m^2 for CPC and PTC DIGESPO collectors, respectively.
The system depicts a natural drop in terms of energy at the beginning of the day. This is due to the thermal losses when sun is not shining (negative value is due to the reference starting point at 0 kWh). The storage temperature starts to increase when irradiation occurs (around 7.10 AM) together with the storage energy value. A small change of the energy storage slope is shows around 12.00AM when the cooking power requirements is at his top. Here, the power required can be higher than the power instantly available from the collector and the thermal storage working as backup is therefore strictly necessary. The large collector area allows a fast increase of the energy loaded through the PCM after lunch time, with a peak in energy available around 3 PM. At this stage the energy stored exceed the energy requirements of a typical day and Figure 11 shows a possible overheating of the PCM material. This suggests that a possible decrease of the thermal storage and collector area can be followed without affecting the thermal behaviour of the system.

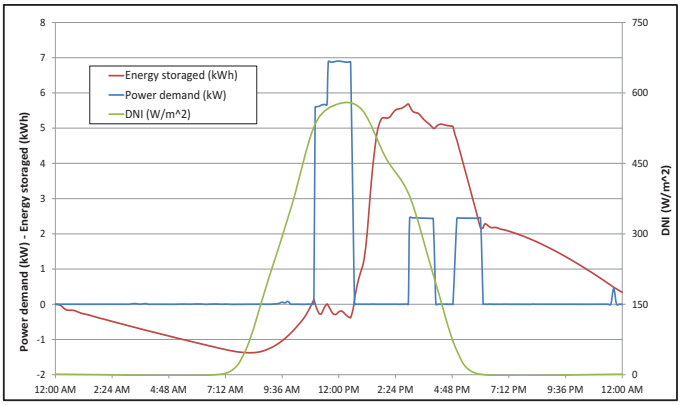

Fig. 12: Scenario 2_Power demand and energy available in the PCM storage

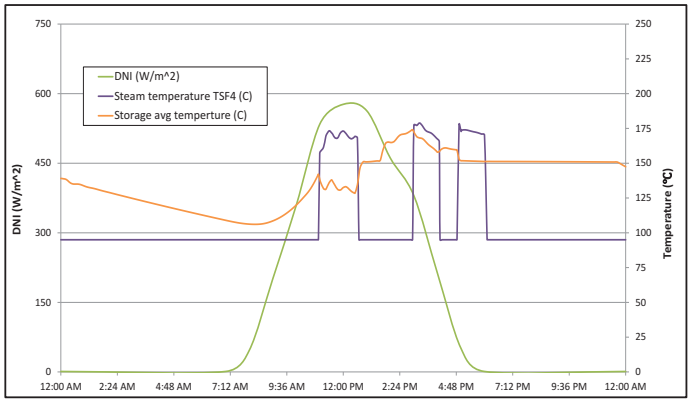

Fig. 13: Scenario 2_ Temperatures of supplied steam and tank average temperature over daily time.

Figure 12 describes the scenario modelled reducing the dimension of the CPC area to 10 m^2 and the storage tank total mass to 70 kg. This configuration seems to satisfy the power demand along a typical day. The maximum peak of energy saved is sufficient to cover the thermal power demand of the hay processing at the end of the day, but an overheating of the phase change material is still depicted in Figure 13.
Outlet steam temperature is strongly dependent by the instant solar irradiation (and therefore by the pressurized water) especially if the storage has not reached the target temperature yet. This behaviour is always true for the cooking power demand, and the highest influence is visible in Figure 13 observing the steam temperature trend. The power demand of the cooking process in fact is required along the morning when the solar radiation has not already refilled the PCM tank. On the other hand, the cooking demand

occurs when the sun is shining and for this reason the power collected is directly exploited by the cooking system and high temperature can be delivered to the cooking pot.
Test showed in chart Figure 13shows a total deployment of the energy stored despite an overheating is still visible in the simulation. Now the possible superheating of the thermal storage simulated does not overpass 190°C as in the previous case but still reaches almost 175°C, over a temperature transition phase of 150°C. This could be reasonably limited reducing the collector area of the power system.

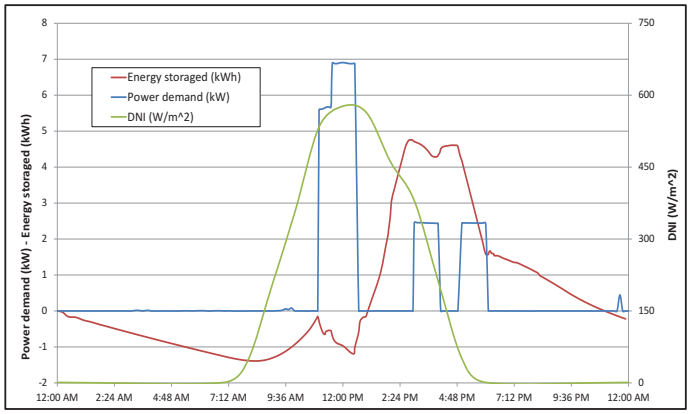

Fig. 14: Scenario 3_Power demand and energy available in the PCM storage

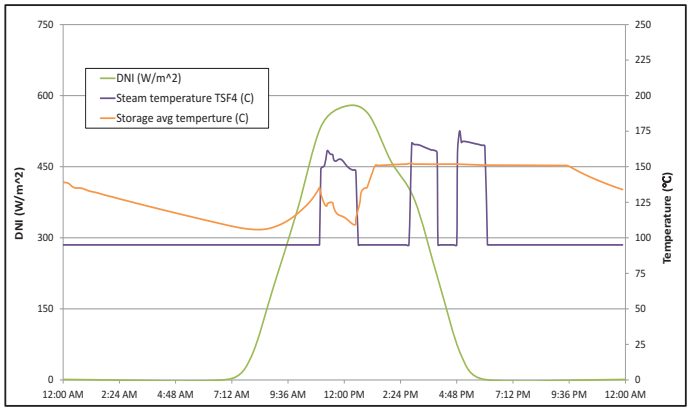

Fig. 15: Scenario 3_ Temperatures of supplied steam and tank average temperature over daily time.

Based on the previous considerations a third scenario is pursued and presented in Figure 14. Here, the total CPC collector area is further reduced. Thermal storage average temperature depicted in graph of Figure 15 does not overpass the PCM transition temperature of 150°C. Obviously, after the sunset a faster temperature drop is now visible. In this scenario the PCM storage works below the design temperature for almost all the typical morning, and a lower steam temperature is expected when lunchtime occurs. This is a second effect related to the CPC area reduction. The average temperature in the storage at 11AM is slightly above 125 °C and dramatically drops below 115°C at the end of the cooking process. This behaviour could affect the cooking effectiveness and reliability of the system, especially if thermal transmission losses on the real installation would be higher than what expected due to poor insulation during the commissioning phase. Moreover, an expected reduction of the optical performances of the solar collectors are normally expected during the lifetime and when used in dusty environments. This, would cause a dramatic decrease of the nominal power available from the collectors with an ulterior effect on the steam production. For these reasons, if the reduction of the collector area certainly reduces the overall economic impact of the system and eliminates PCM's overheating, criticalities regarding the maximum cooking temperature and minimum temperature of the storage are expected.

The last scenario described in Figure 16 further reduces the quantity of PCM material within the storage, keeping the same total collector area of Scenario 3. This reduction deeply affects the economic impact of the thermal storage. The direct consequence is showed in Figure 17. Here, a small peak of overheating is visible in the storage average temperature. Beside this, very low temperature is visible at the end of the day in the thermal tank, suggesting that the new match is not able to satisfy the power requirements. The minimum temperature of the storage tank reached at the end of the day here is much lower than in any other previous case. If this last scenario could show an expected reduction in terms of economic impact the thermal storage cannot be completely exploited, resulting in very low average temperature along the day.

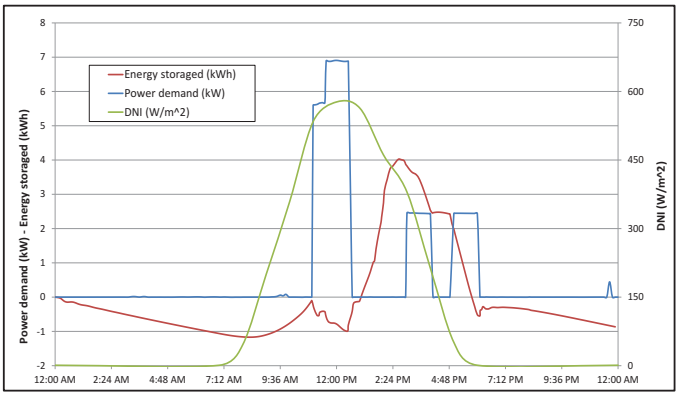

Fig. 16: Scenario 4_Power demand and energy available in the PCM storage

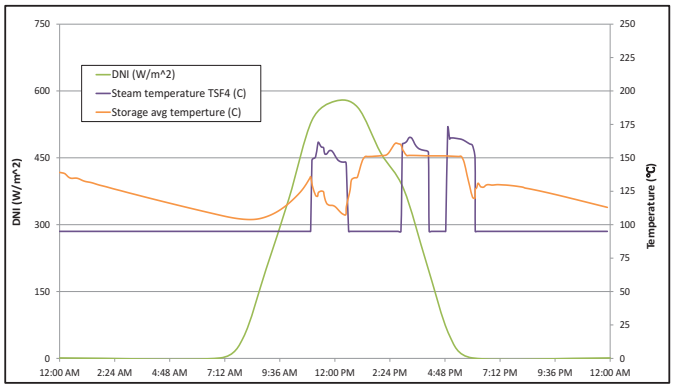

Fig. 17: Scenario 4_ Temperatures of supplied steam and tank average temperature over daily time.

5. Conclusions and Future Works

Dynamic simulations of four different scenarios have been studied in order to properly address the size of solar collectors and PCM thermal storage for a multifunctional rural energy system. The engineering of the system is looking to develop several forms of thermal energy supplied to the school. One of the priorities is a reliable and fossil fuel-free cooking system. Furthermore, the thermal energy accumulated is used during the afternoon to provide high temperature steam to a dedicated hay processing digester. Several technology scenarios have been modelled on a multi objective optimization. Results of the simulations are summarized in Table 2. Scenario 1 shows the best cooking temperature, with an average storage temperature close and stable at 150°C for the most part of the working daily time (a small overheating up to 180°C is visible in the simulation). Due to the large collector area this temperature is rapidly reached at the beginning of the day ensuring reliable temperatures even during the daily cooking activities. Scenario 3 also achieves interesting results. First, a reduction of collectors and PCM material definitely affects the total capital investment. In addition, no overheating is visible in the storage tank and the temperature is constant at 150°C. Despite this, the reduction of collectors' number deeply affects the temperature reached in the storage at the beginning of the cooking time, with dangerous effects on the cooking effectiveness. Scenarios 2 and 4 have been

discharged due to mismatching values between the storage availability and the steam generation temperatures.
Based on these considerations, Scenario 1 is identified and selected as the most reliable solution despite the initial investment cost. At the same time, Scenario 3 could be deeper investigated especially considering the possibility of shifting the cooking habits of the school by 30-45 minutes later in the morning. If agreed with the local community, solar power instantly available could be directly used to satisfy the thermal necessities of the school at lunchtime reducing the necessity of thermal backup. The system could be potentially resized in order to achieve a reduction of costs (reducing the PCM storage) without affecting the performances. This hypothesis may also help to reduce the required dimension of solar collectors, directly affecting the economic investment but maintaining the efficiency and reliability of the system.

Tab. 2: Technical specification of the simulations performed and summary results.

	CPC Area (m^2)	PTC Area (m^2)	PCM total mass (kg)	Max. Energy stored (kWh)	Max Storage avg. temp. (°C)	Min Storage avg. temp. (°C)	Max Steam temp. TSF4 (°C)
Scenario 1 (Fig. 4)	12	3.2	90	7,7	179	108	182
Scenario 2 (Fig. 5)	10	3.2	70	5,6	171	106	177
Scenario 3 (Fig. 6)	7	3.2	70	4,6	150	105	170
Scenario 4 (Fig. 7)	7	3.2	55	4	160	103	169

6. Acknowledgment

Authors acknowledge the support of several activities related to the activity of STAR project. In particular, the FP7-IRP-STAGE STE, grant agreement n° 609837 and the FP7-DIGESPO, grant agreement n° *241267*. The results of the study presented in this paper are part of the ITPAR III bilateral collaboration program between Indian Department of Science and Technology and the Autonomous Province of Trento.

References

1. (Accessed 20.05.2016) http://www.worldometers.info/world-population/india-population/
2. (Accessed 21.09.2016) http://news.bbc.co.uk/2/hi/south_asia/6911544.stm
3. World Economic Outlook. International Monetary Fund (IMF). Retrieved 2014-04-08
4. (Accessed 21.09.2016) University of Washington, Web article: https://artsci.washington.edu/news/2013-10
5. Ashwani Kumar, Kapil Kumar, Naresh Kaushik, Satyawati Sharma, Saroj Mishra. Renewable energy in India: Current status and future potentials. Renwable and Sustainable Energy Reviews, Volume 14, Issue 8, October 2010.
6. (Accessed 21.09.2016) http://www.nistads.res.in/indiasnt2008/t6rural/t6rur85.htm
7. (Accessed 21.09.2016) Ministry on new and renewable energy website: http://www.mnre.gov.in/solar-mission/jnnsm/introduction-2/.
8. (Accessed 21.09.2016) http://solarcooking.wikia.com/wiki/India
9. Tribeni Das, R. Subramanian, A. Chakkaravarthi, Vasudeva Singh, S.Z. Ali, P.K. Bordoloi. Energy conservation in domestic rice cooking. Journal of Food Engineering 75, July 2006.
10. Dilip Kumar De, Muwa Nathaniel, Narendra Nath De, Mathais Ajaeroh Ikechukwu. Cooking rice with minimum energy. Journal of Renewable and Sustainable Energy 6, January 2014.
11. (Accessed 5.04.2016) http://www.digespo.eu/default.aspx.
12. Kuldeep Ojha, Need of independent rural power producers in India – an overview. Journal of Clean Technologies and Environmental Policies, 12, November 2009.
13. J.M. Cabello, J.M. Cejudo, M. Luque, F. Ruiz, K. Deb, R. Tewari Optimization of the size of a solar thermal electricity plant by means of genetic algorithms. Journal of Renewable Energy 36, November 2011.
14. (Accessed 5.09.2016) http://www.paradigmaitalia.it/homepage
15. (Accessed 21.09.2016) http://www.idfa.org/news-views/media-kits/milk/pasteurization.
16. (Accessed 21.06.2016) Weather Data References: SEC, MNRE, Solar Energy Centre, Ministry of New and Renewable Energy, Government of India. http://mnre.gov.in/sec/solarassmnt.htm.

17. (Accessed 5.04.2016) https://www.modelica.org, last access April 2016.
18. Adriano Desideri, Simone Amicabile, Fabrizio Alberti, Silvio Vitali Nari, Sylvain Quoilin, Luigi Crema, Vincent Lemort. Dynamic modeling and control strategies analysis of a novel hybrid small CSP biomass plant for cogeneration applications in building, ISES Solar World Congress 2015, Conference proceeding.
19. Casati, E., Galli, A., Colonna. Thermal energy storage for solar-powered organic Rankine cycle engines. Solar energy 96, October 2013.
20. D. Haillot, T. Bauer∗, U. Kröner, R. Tamme. Thermal analysis of phase change materials in the temperature range 120–150 °C. Joiurnal of Thermochimica Acta 513, 2010.